Can Orbital-Selective Néel Transitions Survive Strong Nonlocal Electronic Correlations?

Evgeny A. Stepanov[1,2,*] and Silke Biermann[1,2,3]
[1]CPHT, CNRS, École polytechnique, Institut Polytechnique de Paris, 91120 Palaiseau, France
[2]Collège de France, Université PSL, 11 place Marcelin Berthelot, 75005 Paris, France
[3]European Theoretical Spectroscopy Facility, 91128 Palaiseau, France

(Received 13 January 2024; accepted 26 April 2024; published 28 May 2024)

Spin- or orbital-selective behaviors in correlated electron materials offer rich promise for spintronics or orbitronics phenomena and applications deriving from them. Strong local electronic Coulomb correlations might lead to an orbital-selective Mott state, characterized by the coexistence of localized electrons in some orbitals with itinerant electrons in others. Nonlocal electronic fluctuations are much more entangled in orbital space than the local ones. For this reason, finding orbital-selective phenomena related to nonlocal correlations, such as orbital-selective magnetic transitions, is a challenge. In this Letter, we investigate possibilities to realize an orbital-selective Néel transition (OSNT). We illustrate that stabilizing this state requires a decoupling of magnetic fluctuations in different orbitals, which can only be realized in the absence of Hund's exchange coupling. On the basis of two-orbital calculations for a Hubbard model with different bandwidths we show that the proposed OSNT can be found all the way from the weak to the strong coupling regime. In the weak coupling regime the transition is governed by a Slater mechanism and thus occurs first for the narrow orbital. At strong coupling a Heisenberg mechanism of the OSNT sets in, and the transition occurs first for the wide orbital. Remarkably, at intermediate values of the interaction we find a nontrivial regime of the OSNT, where the Slater mechanism leads to a Néel transition occurring first for the wide orbital. Our work suggests strategies for searching for orbital-selective Néel ordering in real materials in view of possible spin-orbitronics applications.

DOI: 10.1103/PhysRevLett.132.226501

The most striking effects of electronic Coulomb correlations in strongly correlated materials are probably phase transitions to various ordered states induced by collective electronic behavior. Strong local Coulomb repulsions between electrons favor localization of the electrons on atomic sites and can drive the system toward a Mott-insulating state [1,2]. Nonlocal collective electronic fluctuations are responsible for other types of orderings, in particular magnetic or superconducting states. In multiorbital systems, the orbital degrees of freedom not only have the potential to enhance these effects but can also enable the emergence of nontrivial states of matter that cannot be realized in the single-orbital case. Celebrated examples are orbital-selective states characterized by the coexistence of radically different collective electronic behaviors associated with distinct orbitals. Such phenomena have attracted tremendous attention since the experimental observation of non-Fermi liquid behavior in the resistivity and an enhanced spin susceptibility in the metallic phase of the doped ($0.2 < x < 0.5$) ruthenate $Ca_{2-x}Sr_xRuO_4$ [3]. The material was suggested to undergo an orbital-selective metal-insulator transition (OSMIT) to a phase, where itinerant electrons in some orbitals coexist with localized electrons living in other orbitals [4]. Such "orbital-selective Mott transitions" have instantaneously become a hot topic of condensed matter physics, triggering enormous excitement not only for ruthenate compounds [5–11], but also for iron-based superconductors [12–15], iron chalcogenides [16–18], and the Van der Waals ferromagnet $Fe_{3-x}GeTe_2$ [19]. The link between theoretical findings in model systems [4,20–58] and observations in real materials remains, however, controversial, even more so as the orbital-selective Mott phase is a rather fragile state that is unstable against both local [59] and nonlocal [60] interorbital hopping processes and can also be destroyed by strong magnetic fluctuations [61].

Because of technical limitations, the overwhelming majority of theoretical studies so far have focused on the formation of a paramagnetic Mott state, driven by local electronic correlations. Likely more relevant to real materials questions at low temperatures are an entirely different kind of orbital-selective phases, which are states originating from orbital-selective magnetic fluctuations, and in the extreme case magnetic orderings. Speculations about the existence of such states have been spurred on by the vast literature on iron-based superconducting materials [62–72], but to date no strategy for realizing even the simplest orbital-selective Néel phase has been established. Doing so requires using advanced theoretical methods that go beyond local approximations. Taking into account spatial collective electronic fluctuations in a multiorbital framework is computationally demanding, which greatly limits

possibilities of studying OSMITs to a symmetry-broken magnetic state [47–58]. Nonlocal collective electronic fluctuations that would drive the magnetic OSMIT are strongly entangled in orbital space [61,73], which additionally complicates realizing the orbital-selective magnetic state. Existing theoretical studies of magnetic OSMITs mostly start from models that assume the existence of a local magnetic moment, which is then explicitly introduced in the theoretical description [47–53]. While giving interesting insights into the consequences of orbital-selective magnetic moments, such approaches do not allow one to decide on their existence. On the contrary, it has been shown recently that the ordered magnetic state is formed simultaneously within all orbitals that are coupled by the local interorbital exchange interaction (Hund's rule coupling) [61].

There are only few works, where the OSMIT to the ordered magnetic state was addressed more accurately based on interacting electronic models [54–57]. In this set of works the authors performed dynamical mean-field theory (DMFT) [74] or mean-field calculations for a two-orbital Hubbard model on a square lattice. Various ordered magnetic states were investigated either by introducing two sublattices or within the dynamical cluster approximation [75]. The authors argue that having distinct band dispersions for different orbitals is crucial for realizing the OSMIT to the ordered magnetic state, and the proposed mechanism is not sensitive to the strength of the Hund's coupling J [56]. Interestingly, this conclusion seems to be in contradiction with the absence of an OSNT found recently in a similar system in the case of a finite Hund's coupling J [61].

In this Letter using an advanced many-body approach that includes spatial fluctuations beyond DMFT, we propose a mechanism for the orbital-selective Néel transition (OSNT) that can be realized in a system with different bandwidths in the absence of Hund's coupling for an arbitrarily strong local Coulomb interaction. We find that the OSNT occurs differently in the weak and strong-coupling regimes, which can be associated respectively with the Slater and Heisenberg mechanisms of the Néel transition. Interestingly, despite the absence of Hund's coupling, the electrons in different orbitals still do interact by means of the interorbital local Coulomb potential. This interaction manifests itself in the Kondo screening of the local magnetic moment of the narrow orbital by itinerant electrons of the wide orbital, which results in a simultaneous formation of the local moment in both orbitals.

Model and method.—We consider a half-filled two-orbital Hubbard model on a cubic lattice described by the Hamiltonian

$$H = \sum_{jj',l,\sigma} t^{l}_{jj'} c^{\dagger}_{jl\sigma} c_{j'l\sigma} + \frac{1}{2} \sum_{j,\{l\},\sigma\sigma'} U_{l_1 l_2 l_3 l_4} c^{\dagger}_{jl_1\sigma} c^{\dagger}_{jl_2\sigma'} c_{jl_4\sigma'} c_{jl_3\sigma},$$

where $c^{(\dagger)}_{jl\sigma}$ is the annihilation (creation) operator for an electron on the lattice site j, in orbital $l \in \{1,2\}$, with spin projection $\sigma \in \{\uparrow,\downarrow\}$. $t^{l}_{jj'}$ is the intraorbital (l) hopping amplitude between sites j and j'. We restrict ourselves to nearest-neighbor hoppings, and choose the half-bandwidth of the narrow band as our unit of energy, i.e., $t^{1}_{jj'} = 1/6$. The second band is double as wide with $t^{2}_{jj'} = 1/3$. The interaction is parametrized in the Kanamori form that includes the intraorbital $U_{llll} = U$, interorbital $U_{ll'll'} = U - 2J$, spin flip $U_{ll'l'l} = J$, and pair hopping $U_{lll'l'} = J$ terms. J is the Hund's rule coupling.

An accurate description of the Néel transition requires accounting for long-range magnetic fluctuations and their influence on the electronic excitations (see, e.g., Refs. [76–78] and references therein). In the multiorbital framework both of these aspects can be consistently taken into account by an advanced many-body approach dubbed "dual triply irreducible local expansion" (D-TRILEX) [79–81], which extends the "TRILEX" approach of Refs. [82,83] to the dual fermion [84–87] and boson [88–96] variables. In this method, nonlocal collective electronic fluctuations are treated self-consistently [97–100] by performing a diagrammatic expansion around DMFT [101,102]. A decisive advantage of the D-TRILEX method is its rather simple diagrammatic structure, which facilitates tractable numerical calculations within a multiorbital framework [61,73,103,104]. Crucially, despite its relative simplicity, D-TRILEX maintains the same level of accuracy as significantly more complex diagrammatic approaches, providing good results for both single and two-particle observables [80,81] and especially for the Néel temperature (See Fig. 6.13 in [78]) relevant for the current work.

Results.—We have first performed D-TRILEX calculations for the two-orbital Hubbard model in the absence of Hund's coupling ($J = 0$). We calculate the orbital-selective Néel temperatures (T_N) by identifying the divergences of the orbital components of the static ($\omega = 0$) spin susceptibility $X^{sp}_{ll'}(\mathbf{q},\omega) = \langle m^{z}_{\mathbf{q},\omega,l} m^{z}_{-\mathbf{q},-\omega,l'} \rangle$ obtained at the antiferromagnetic (AFM) wave vector $\mathbf{Q} = \{\pi,\pi,\pi\}$ [61]. Here, $m^{z}_{\mathbf{q},\omega,l} = \sum_{\mathbf{k},\nu,\sigma} c^{\dagger}_{\mathbf{k}+\mathbf{q},\nu+\omega,l,\sigma} \sigma^{z}_{\sigma\sigma} c_{\mathbf{k},\nu,l,\sigma}$, and σ^z is the familiar Pauli matrix. Details of the calculations are presented in the Supplemental Material (SM) [105]. The results are summarized in Fig. 1.

In the weak-coupling regime ($U < 1.95$) upon lowering the temperature the $l = 1$ (narrow orbital) component of the AFM susceptibility diverges first, while the $l = 2$ (wide orbital) component remains finite at the transition point. This behavior indicates the OSNT to a phase, where electrons in the narrow orbital order antiferromagnetically, while the wide orbital stays itinerant. At $U > 1.95$ we observe the opposite situation: the transition to the ordered AFM state occurs first for the wide orbital, while the narrow orbital remains itinerant. Remarkably, the system exhibits

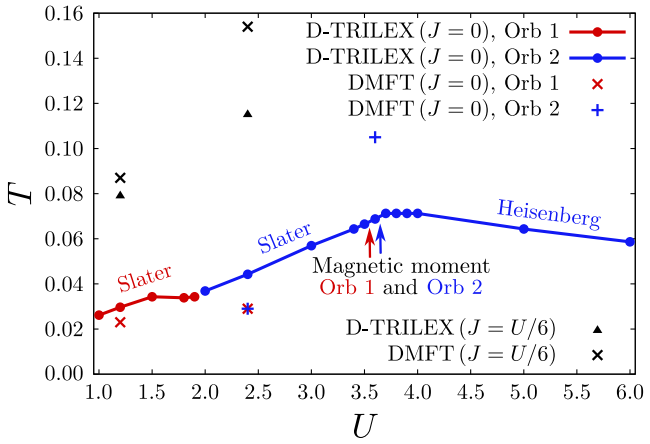

FIG. 1. Néel temperature for the two-orbital half-filled Hubbard model on a cubic lattice with different bandwidths of the two orbitals. Results are obtained using D-TRILEX and DMFT for different values of the Hund's exchange coupling J. At finite J the Néel transition occurs simultaneously for both orbitals (black "triangle" and "cross" markers). The OSNT scenario is realized in the absence of J: at $U < 1.95$ upon decreasing the temperature the Néel transition occurs first for the narrow orbital (Orb 1, red color), and at $U > 1.95$ for the wide orbital (Orb 2, blue color). Critical interactions at which the local magnetic moment is formed above the Néel transition are indicated by arrows.

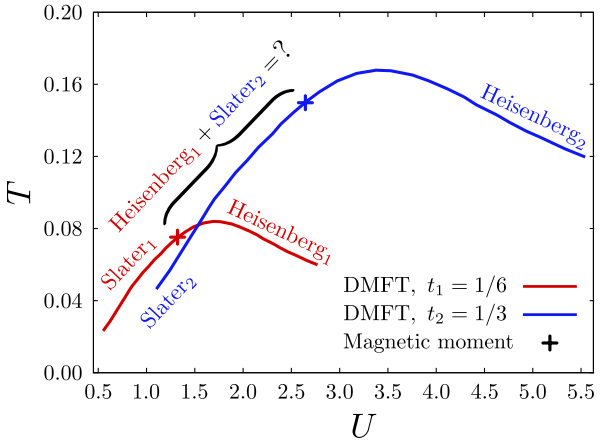

FIG. 2. Sketch of the proposed mechanism for the OSNT. Red and blue curves show the Néel phase boundaries predicted by DMFT for a half-filled single-band Hubbard model on a cubic lattice as a function of the local interaction strength U. Results are taken from Ref. [112] and rescaled to get the phase boundaries for two different bandwidths defined by the nearest-neighbor hopping amplitudes $t_1 = 1/6$ (red) and $t_2 = 1/3$ (blue). "+" markers indicate the point on each phase boundary at which the local magnetic moment is formed (see Ref. [96]), which separates the Slater (at smaller U) and Heisenberg (at larger U) regimes of the Néel transition.

an OSNT for any value of the interaction, except for $U \simeq 1.95$ where $T_{N_1} = T_{N_2}$.

We now argue that the choice of vanishing Hund's coupling made above is essential for these results. Indeed, in a multiorbital system magnetic fluctuations of different orbitals are coupled due to the presence of Hund's exchange coupling J. This coupling is realized through interorbital three-point (Hedin [106]) vertex corrections that are present in the self-energy and the polarization operator for any finite value of J. These vertices connect the renormalized interaction in the spin channel to the electronic Green's function and thus are responsible for mixing different orbital contributions to the spin susceptibility. Strong spatial magnetic fluctuations enhance this mixing, which leads to a simultaneous Néel transition for different orbitals [61]. Therefore, realizing the OSNT necessarily requires magnetic fluctuations of different orbitals to decouple. This happens in the absence of Hund's coupling, since in this case the interorbital components of the vertex function in the spin channel are identically zero. In realistic materials, the Hund's coupling can be suppressed, e.g., through the Jahn-Teller effect of phonons, which, as has been demonstrated for fullerides, can result even in a sign change of J [107–111].

Since at $J = 0$ magnetic fluctuations of different orbitals decouple, the proposed mechanism of the OSNT can be qualitatively illustrated on the basis of single-orbital calculations. Let us consider two separate single-orbital Hubbard models on a cubic lattice with different bandwidths defined by the nearest-neighbor hoppings $t_1 = 1/6$ (narrow orbital) and $t_2 = 1/3$ (wide orbital). In Fig. 2 we compare the Néel temperatures for these two models as a function of the interaction U. The Néel phase boundaries for the narrow (red) and wide (blue) orbitals are obtained by rescaling the results of DMFT calculations taken from Ref. [112].

Figure 2 demonstrates that in the weak coupling regime the Néel temperature of the narrow orbital is larger than the Néel temperature of the wide orbital ($T_{N_1} > T_{N_2}$). However, in the strong coupling regime the relation between the Néel temperatures is opposite, namely $T_{N_1} < T_{N_2}$. This result can be explained by the fact that in the Slater regime of magnetic fluctuation T_N increases with increasing interaction. For a given value of U, the ratio U over the bandwidth, U/W, is stronger for the narrow orbital, which results in a higher T_N for this orbital at weak coupling. In contrast, in the Heisenberg (strong-coupling) regime the Néel temperature is determined by the exchange interaction $T_N \sim t^2/U$, and the latter is larger for the wide orbital.

These two regimes of magnetic fluctuations can be distinguished by the absence (Slater) or presence (Heisenberg) of a local magnetic moment in the system. In the single-orbital Hubbard model the formation of the local magnetic moment has been studied in Ref. [96]. The critical point at the Néel phase boundary, where the local magnetic moment starts to form prior to the transition, is depicted in Fig. 2 by "+" markers. It occurs close to the top

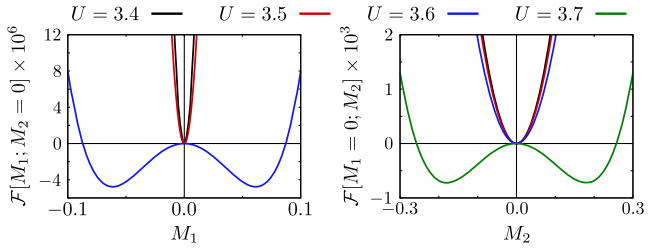

FIG. 3. Local free energy $\mathcal{F}[M_1; M_2]$ as a function of the value of one of the two local magnetic moments M_1 (Orb 1, left panel) and M_2 (Orb 2, left panel) obtained along the Néel phase boundary. The transition from a parabolic form of the free energy to a double-well potential form signals the formation of the local magnetic moment, which for both orbitals occurs approximately at the same value of the interaction $U = 3.55$ (Orb 1) $U_2 = 3.65$ (Orb 2).

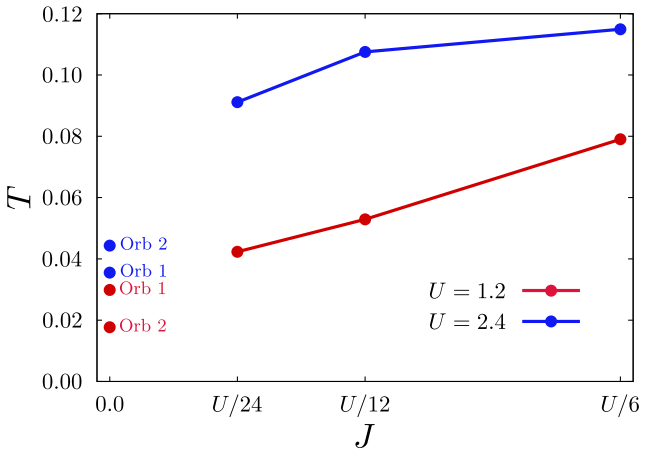

FIG. 4. Néel temperature as a function of the Hund's coupling J. Model parameters are the same as in Fig. 1. Results are obtained using D-TRILEX for $U = 1.2$ (red) and $U = 2.4$ (blue). At $J = 0$ the system displays the OSNT with different Néel temperatures for the two orbitals indicated by "Orb 1" and "Orb 2" labels.

of each dome-shaped curve. Remarkably, at intermediate couplings ($1.5 \lesssim U \lesssim 2.7$) one may expect a nontrivial regime, where the Néel transition occurs first for the wide orbital, where the local magnetic moment is not formed yet, while the narrow orbital remains itinerant but exhibiting a local moment.

To distinguish between the Slater and Heisenberg mechanisms of the OSNT we perform calculations for the local magnetic moment along the lines of Ref. [96]: Excluding the contribution of the itinerant electrons, we study the local free energy $\mathcal{F}[M_1; M_2]$, which is associated with the behavior of the local magnetic moment M_1 and M_2 of each orbital (for details see Ref. [96]). Because of to the decoupling of the magnetic fluctuations in the two orbitals, the free energy takes the form $\mathcal{F}[M_1;M_2]=\mathcal{F}[M_1]+\mathcal{F}[M_2]$. The corresponding result for the free energy obtained along the Néel phase boundary is shown in Fig. 3. Remarkably, despite the decoupling, the local magnetic moment in both orbitals is formed almost at the same point at the Néel phase boundary ($U_1 = 3.55$ for Orb 1 and $U_1 = 3.65$ for Orb 2) as depicted by arrows in Fig. 1). This effect cannot be explained by a single-band picture that does not account for the interorbital Coulomb interaction $U_{ll'll'}$. This interaction does not couple the magnetic fluctuations of different orbitals but is responsible for spin-flip processes that couple different orbitals. These processes allow for Kondo screening of the local magnetic moment, which otherwise would have been formed at the narrow orbital at smaller values of U by itinerant electronic fluctuations of the wide orbital. As a result, in the intermediate coupling regime the OSNT is governed by the Slater mechanism, although the Néel transition first occurs for the wide orbital and not for the narrow orbital as in the weak-coupling case.

To complete the story, we also perform AFM (two-sublattice) DMFT calculations for $J = 0$. In this case, in the weak-coupling regime, the Néel transition occurs first for the narrow orbital ($T_N = 0.023$, $U = 1.2$, red "×" marker in Fig. 1) and at larger values of the interaction—for the wide orbital ($T_N = 0.105$, $U = 3.6$, blue "+" marker in Fig. 1). The two Néel temperatures coincide at $T = 0.029$ and $U = 2.4$. We observe that at small values of the interaction DMFT underestimates the transition temperature, and the crossing point $T_{N_1} = T_{N_2}$ is shifted to smaller temperature and larger U compared to the D-TRILEX result. At larger interaction U DMFT strongly overestimates the transition temperature.

In addition, we perform both DMFT and D-TRILEX calculations for a nonzero value of the Hund's coupling $J = U/6$. As expected from Ref. [61], in this case the OSNT transforms into an ordinary Néel transition that occurs simultaneously for both orbitals. The corresponding Néel temperatures are shown in Fig. 1 for $U = 1.2$ and $U = 2.4$ by black "▲" (D-TRILEX) and black "×" (DMFT) markers. We find that at both interaction strengths DMFT predicts higher Néel temperatures compared to D-TRILEX, which is consistent with single-orbital calculations [76–78]. To provide more insights into how the Hund's coupling destroys the OSNT, in Fig. 4 we show the evolution of the Néel temperature as a function of J. As expected, at weak coupling ($U = 1.2$, red curve) T_N depends almost linearly on J, while at larger interactions ($U = 2.4$, blue curve) deviations start to show. The OSNT scenario is realized only in the absence of Hund's coupling, where the two orbitals have different Néel temperatures labeled as "Orb 1" and "Orb 2" in Fig. 4. Nevertheless, as we demonstrate in SM [105], in the $J \neq 0$ case the spin susceptibilities of the two orbitals also become different above the Néel transition. At larger values of J the difference between the two susceptibilities is smaller because Hund's coupling causes a mixing of contributions of different orbitals [73]. Upon decreasing J the difference

between the susceptibilities increases and they become similar only in the vicinity of the Néel transition. At $J = 0$ the mixing between the two orbital components disappears, which eventually leads to the OSNT.

These findings motivate us to study the influence of long-range magnetic fluctuations on the magnetic OSMIT proposed previously in Ref. [56] on the basis of DMFT calculations. Here, we consider a two-orbital Hubbard model on a square lattice with nearest-neighbor $t_1 = t_2 = 1$ and next-nearest-neighbor $t'_1 = 1$, $t'_2 = 0$ hopping amplitudes, Coulomb interaction $U = 4$, and Hund's coupling $J = 1$. Within DMFT, for this set of model parameters the system lies well in the orbital-selective phase, characterized by localized Néel AFM behavior for the $l = 1$ orbital, while the $l = 2$ orbital remains itinerant [56]. Within D-TRILEX, on the contrary, for this set of model parameters we do not observe any signature of an OSMIT, in line with the above findings and Ref. [61]. Instead, within D-TRILEX we observe a conventional (non-orbital-selective) Néel transition that occurs simultaneously for both orbitals. Indeed, in SM [105] we show that both orbital components of the AFM susceptibility diverge at the same critical temperature $T_N \simeq 0.1$. The absence of the orbital-selective phase is thus due to the effect of long-range electronic correlations not captured in the cluster DMFT calculations of Refs. [54–57].

Conclusions.—In this Letter, we have established strategies for realizing orbital-selective Néel-ordered magnetic states. We have demonstrated that in the absence of Hund's exchange coupling J the two-orbital Hubbard model with different bandwidths can indeed undergo an OSNT at any interaction strength (except one specific value of the interaction). Remarkably, the OSNT occurs differently in the weak and strong-coupling regimes of interaction. In the weak-coupling regime it is governed by a Slater mechanism, namely in the absence of a local magnetic moment. Consequently, the Néel transition occurs first for the narrow orbital, while the wide orbital remains itinerant. In the strong-coupling regime, a local magnetic moment is formed, and the Heisenberg mechanism of the OSNT leads to localized behavior occurring first in the wide orbital, while the narrow orbital stays itinerant. Interestingly, at intermediate couplings we have found a nontrivial regime, where the transition occurs first for the wide orbital, but the local magnetic moment is not yet formed. The latter is Kondo screened by electronic fluctuations of the wide orbitals. This results in a Slater mechanism of the OSNT at intermediate interaction strengths. Most intriguingly, in the presence of Hund's coupling the OSNT is destroyed altogether: Hund's exchange effectively couples orbital degrees of freedom, and is thus detrimental to orbital-selective behavior. The ubiquity of Hund's exchange in real materials may provide a natural explanation for OSNTs likely being rather the exception than the rule. Nevertheless, a systematic search for OSNT in real materials might prove worthwhile in view of potential applications in spintronics devices, e.g., for memory applications, spin valves, or spin-charge converters. Our work strongly suggests a materials screening among materials with as low as possible Hund's exchange coupling. A trivial corollary of this argument is obtained by replacing orbital indices by site indices: thanks to the intrinsically weak direct intersite exchange interaction, site-selective magnetic orderings in materials with several correlated sites per unit cell should be found more easily than orbital-selective OSNTs.

The authors acknowledge support from IDRIS/GENCI Orsay under Project No. A0130901393 and the help of the CPHT computer support team.

*Corresponding author: evgeny.stepanov@polytechnique.edu

[1] N. F. Mott, *Metal-Insulator Transitions* (Taylor & Francis, London, 1974).

[2] Masatoshi Imada, Atsushi Fujimori, and Yoshinori Tokura, Metal-insulator transitions, Rev. Mod. Phys. **70**, 1039 (1998).

[3] S. Nakatsuji and Y. Maeno, Quasi-two-dimensional Mott transition system $Ca_{2-x}Sr_xRuO_4$, Phys. Rev. Lett. **84**, 2666 (2000).

[4] V. I. Anisimov, I. A. Nekrasov, D. E. Kondakov, T. M. Rice, and M. Sigrist, Orbital-selective Mott-insulator transition in $Ca_{2-x}Sr_xRuO_4$, Eur. Phys. J. B **25**, 191 (2002).

[5] S. Nakatsuji, D. Hall, L. Balicas, Z. Fisk, K. Sugahara, M. Yoshioka, and Y. Maeno, Heavy-mass Fermi liquid near a ferromagnetic instability in layered ruthenates, Phys. Rev. Lett. **90**, 137202 (2003).

[6] S.-C. Wang, H.-B. Yang, A. K. P. Sekharan, S. Souma, H. Matsui, T. Sato, T. Takahashi, Chenxi Lu, Jiandi Zhang, R. Jin, D. Mandrus, E. W. Plummer, Z. Wang, and H. Ding, Fermi surface topology of $Ca_{1.5}Sr_{0.5}RuO_4$ determined by angle-resolved photoelectron spectroscopy, Phys. Rev. Lett. **93**, 177007 (2004).

[7] L. Balicas, S. Nakatsuji, D. Hall, T. Ohnishi, Z. Fisk, Y. Maeno, and D. J. Singh, Severe Fermi surface reconstruction at a metamagnetic transition in $Ca_{2-x}Sr_xRuO_4$ (for $0.2 \leq x \leq 0.5$), Phys. Rev. Lett. **95**, 196407 (2005).

[8] J. S. Lee, S. J. Moon, T. W. Noh, S. Nakatsuji, and Y. Maeno, Orbital-selective mass enhancements in multiband $Ca_{2-x}Sr_xRuO_4$ systems analyzed by the extended Drude model, Phys. Rev. Lett. **96**, 057401 (2006).

[9] B. J. Kim, Jaejun Yu, H. Koh, I. Nagai, S. I. Ikeda, S.-J. Oh, and C. Kim, Missing xy-band Fermi surface in $4d$ transition-metal oxide Sr_2RhO_4: Effect of the octahedra rotation on the electronic structure, Phys. Rev. Lett. **97**, 106401 (2006).

[10] A. Shimoyamada, K. Ishizaka, S. Tsuda, S. Nakatsuji, Y. Maeno, and S. Shin, Strong mass renormalization at a local momentum space in multiorbital $Ca_{1.8}Sr_{0.2}RuO_4$, Phys. Rev. Lett. **102**, 086401 (2009).

[11] M. Neupane, P. Richard, Z.-H. Pan, Y.-M. Xu, R. Jin, D. Mandrus, X. Dai, Z. Fang, Z. Wang, and H. Ding,

Observation of a novel orbital selective Mott transition in $Ca_{1.8}Sr_{0.2}RuO_4$, Phys. Rev. Lett. **103**, 097001 (2009).
[12] M. Yi, D. H. Lu, R. Yu, S. C. Riggs, J.-H. Chu, B. Lv, Z. K. Liu, M. Lu, Y.-T. Cui, M. Hashimoto, S.-K. Mo, Z. Hussain, C. W. Chu, I. R. Fisher, Q. Si, and Z.-X. Shen, Observation of temperature-induced crossover to an orbital-selective Mott phase in $A_xFe_{2-y}Se_2$ (A=K, Rb) superconductors, Phys. Rev. Lett. **110**, 067003 (2013).
[13] P. Dai, J. Hu, and E. Dagotto, Magnetism and its microscopic origin in iron-based high-temperature superconductors, Nat. Phys. **8**, 709 (2012).
[14] Ming Yi, Yan Zhang, Zhi-Xun Shen, and Donghui Lu, Role of the orbital degree of freedom in iron-based superconductors, npj Quantum Mater. **2**, 57 (2017).
[15] Rong Yu, Haoyu Hu, Emilian M. Nica, Jian-Xin Zhu, and Qimiao Si, Orbital selectivity in electron correlations and superconducting pairing of iron-based superconductors, Front. Phys. **9**, 578347 (2021).
[16] Ming Yi *et al.*, Observation of universal strong orbital-dependent correlation effects in iron chalcogenides, Nat. Commun. **6**, 7777 (2015).
[17] Jianwei Huang *et al.*, Correlation-driven electronic reconstruction in $FeTe_{1-x}Se_x$, Commun. Phys. **5**, 29 (2022).
[18] Minjae Kim, Sangkook Choi, Walber Hugo Brito, and Gabriel Kotliar, Orbital selective Mott transition effects and non-trivial topology of iron chalcogenide, Phys. Rev. Lett. **132**, 136504 (2024).
[19] Xiaojian Bai, Frank Lechermann, Yaohua Liu, Yongqiang Cheng, Alexander I. Kolesnikov, Feng Ye, Travis J. Williams, Songxue Chi, Tao Hong, Garrett E. Granroth, Andrew F. May, and Stuart Calder, Antiferromagnetic fluctuations and orbital-selective Mott transition in the van der Waals ferromagnet $Fe_{3-x}GeTe_2$, Phys. Rev. B **106**, L180409 (2022).
[20] Zhong Fang, Naoto Nagaosa, and Kiyoyuki Terakura, Orbital-dependent phase control in $Ca_{2-x}Sr_xRuO_4$ ($0 < \sim x < \sim 0.5$), Phys. Rev. B **69**, 045116 (2004).
[21] Akihisa Koga, Norio Kawakami, T. M. Rice, and Manfred Sigrist, Orbital-selective Mott transitions in the degenerate Hubbard model, Phys. Rev. Lett. **92**, 216402 (2004).
[22] Akihisa Koga, Norio Kawakami, T. M. Rice, and Manfred Sigrist, Spin, charge, and orbital fluctuations in a multiorbital Mott insulator, Phys. Rev. B **72**, 045128 (2005).
[23] C. Knecht, N. Blümer, and P. G. J. van Dongen, Orbital-selective Mott transitions in the anisotropic two-band Hubbard model at finite temperatures, Phys. Rev. B **72**, 081103(R) (2005).
[24] R. Arita and K. Held, Orbital-selective Mott-Hubbard transition in the two-band Hubbard model, Phys. Rev. B **72**, 201102(R) (2005).
[25] L. de'Medici, A. Georges, and S. Biermann, Orbital-selective Mott transition in multiband systems: Slave-spin representation and dynamical mean-field theory, Phys. Rev. B **72**, 205124 (2005).
[26] Michel Ferrero, Federico Becca, Michele Fabrizio, and Massimo Capone, Dynamical behavior across the Mott transition of two bands with different bandwidths, Phys. Rev. B **72**, 205126 (2005).
[27] A. Liebsch, Novel Mott transitions in a nonisotropic two-band Hubbard model, Phys. Rev. Lett. **95**, 116402 (2005).
[28] S. Biermann, L. de' Medici, and A. Georges, Non-Fermi-liquid behavior and double-exchange physics in orbital-selective Mott systems, Phys. Rev. Lett. **95**, 206401 (2005).
[29] Kensuke Inaba and Akihisa Koga, Phase diagrams of the two-orbital Hubbard model with different bandwidths, Phys. Rev. B **73**, 155106 (2006).
[30] Philipp Werner and Andrew J. Millis, High-spin to low-spin and orbital polarization transitions in multiorbital Mott systems, Phys. Rev. Lett. **99**, 126405 (2007).
[31] T. A. Costi and A. Liebsch, Quantum phase transition in the two-band Hubbard model, Phys. Rev. Lett. **99**, 236404 (2007).
[32] Philipp Werner, Emanuel Gull, and Andrew J. Millis, Metal-insulator phase diagram and orbital selectivity in three-orbital models with rotationally invariant Hund coupling, Phys. Rev. B **79**, 115119 (2009).
[33] Luca de' Medici, S. R. Hassan, Massimo Capone, and Xi Dai, Orbital-selective Mott transition out of band degeneracy lifting, Phys. Rev. Lett. **102**, 126401 (2009).
[34] K. Bouadim, G. G. Batrouni, and R. T. Scalettar, Determinant quantum Monte Carlo study of the orbitally selective Mott transition, Phys. Rev. Lett. **102**, 226402 (2009).
[35] Eberhard Jakobi, Nils Blümer, and Peter van Dongen, Orbital-selective Mott transitions in a doped two-band Hubbard model, Phys. Rev. B **80**, 115109 (2009).
[36] Y. Song and L.-J. Zou, Two-orbital systems with crystal field splitting and interorbital hopping, Eur. Phys. J. B **72**, 59 (2009).
[37] Hunpyo Lee, Yu-Zhong Zhang, Harald O. Jeschke, Roser Valentí, and Hartmut Monien, Dynamical cluster approximation study of the anisotropic two-orbital Hubbard model, Phys. Rev. Lett. **104**, 026402 (2010).
[38] Yi-Zhuang You, Fan Yang, Su-Peng Kou, and Zheng-Yu Weng, Phase diagram and a possible unified description of intercalated iron selenide superconductors, Phys. Rev. Lett. **107**, 167001 (2011).
[39] Luca de' Medici, Hund's coupling and its key role in tuning multiorbital correlations, Phys. Rev. B **83**, 205112 (2011).
[40] Tomoko Kita, Takuma Ohashi, and Norio Kawakami, Mott transition in three-orbital Hubbard model with orbital splitting, Phys. Rev. B **84**, 195130 (2011).
[41] Li Huang, Liang Du, and Xi Dai, Complete phase diagram for three-band Hubbard model with orbital degeneracy lifted by crystal field splitting, Phys. Rev. B **86**, 035150 (2012).
[42] E. Bascones, B. Valenzuela, and M. J. Calderón, Orbital differentiation and the role of orbital ordering in the magnetic state of Fe superconductors, Phys. Rev. B **86**, 174508 (2012).
[43] Rong Yu and Qimiao Si, Orbital-selective Mott phase in multiorbital models for alkaline iron selenides $\mathbf{K}_{1-x}Fe_{2-y}Se_2$, Phys. Rev. Lett. **110**, 146402 (2013).
[44] Luca de' Medici, Gianluca Giovannetti, and Massimo Capone, Selective Mott physics as a key to iron superconductors, Phys. Rev. Lett. **112**, 177001 (2014).

[45] Yilin Wang, Li Huang, Liang Du, and Xi Dai, Doping-driven orbital-selective Mott transition in multi-band Hubbard models with crystal field splitting, Chin. Phys. B **25**, 037103 (2016).
[46] Fabian B. Kugler, Seung-Sup B. Lee, Andreas Weichselbaum, Gabriel Kotliar, and Jan von Delft, Orbital differentiation in Hund metals, Phys. Rev. B **100**, 115159 (2019).
[47] Jiansheng Wu, Philip Phillips, and A. H. Castro Neto, Theory of the magnetic moment in iron pnictides, Phys. Rev. Lett. **101**, 126401 (2008).
[48] Andreas Hackl and Matthias Vojta, Pressure-induced magnetic transition and volume collapse in FeAs superconductors: An orbital-selective Mott scenario, New J. Phys. **11**, 055064 (2009).
[49] Su-Peng Kou, Tao Li, and Zheng-Yu Weng, Coexistence of itinerant electrons and local moments in iron-based superconductors, Europhys. Lett. **88**, 17010 (2009).
[50] Wei-Guo Yin, Chi-Cheng Lee, and Wei Ku, Unified picture for magnetic correlations in iron-based superconductors, Phys. Rev. Lett. **105**, 107004 (2010).
[51] Fan Yang, Su-Peng Kou, and Zheng-Yu Weng, Collective spin mode in a multicomponent system of coupled itinerant and localized electrons, Phys. Rev. B **81**, 245130 (2010).
[52] Weicheng Lv, Frank Krüger, and Philip Phillips, Orbital ordering and unfrustrated $(\pi, 0)$ magnetism from degenerate double exchange in the iron pnictides, Phys. Rev. B **82**, 045125 (2010).
[53] Yi-Zhuang You, Fan Yang, Su-Peng Kou, and Zheng-Yu Weng, Magnetic and superconducting instabilities in a hybrid model of itinerant/localized electrons for iron pnictides, Phys. Rev. B **84**, 054527 (2011).
[54] Hunpyo Lee, Yu-Zhong Zhang, Harald O. Jeschke, and Roser Valentí, Possible origin of the reduced ordered magnetic moment in iron pnictides: A dynamical mean-field theory study, Phys. Rev. B **81**, 220506(R) (2010).
[55] Hunpyo Lee, Yu-Zhong Zhang, Harald O. Jeschke, and Roser Valentí, Orbital-selective phase transition induced by different magnetic states: A dynamical cluster approximation study, Phys. Rev. B **84**, 020401(R) (2011).
[56] Yu-Zhong Zhang, Hunpyo Lee, Hai-Qing Lin, Chang-Qin Wu, Harald O. Jeschke, and Roser Valentí, General mechanism for orbital selective phase transitions, Phys. Rev. B **85**, 035123 (2012).
[57] Yao Yao, Yu-Zhong Zhang, Hunpyo Lee, Harald O Jeschke, Roser Valenti, Hai-Qing Lin, and Chang-Qin Wu, Orbital selective phase transition, Mod. Phys. Lett. B **27**, 1330015 (2013).
[58] Ying Ran, Fa Wang, Hui Zhai, Ashvin Vishwanath, and Dung-Hai Lee, Nodal spin density wave and band topology of the FeAs-based materials, Phys. Rev. B **79**, 014505 (2009).
[59] L. de' Medici, A. Georges, G. Kotliar, and S. Biermann, Mott transition and Kondo screening in f-electron metals, Phys. Rev. Lett. **95**, 066402 (2005).
[60] Fabian B. Kugler and Gabriel Kotliar, Is the orbital-selective Mott phase stable against interorbital hopping?, Phys. Rev. Lett. **129**, 096403 (2022).
[61] Evgeny A. Stepanov, Eliminating orbital selectivity from the metal-insulator transition by strong magnetic fluctuations, Phys. Rev. Lett. **129**, 096404 (2022).
[62] T. Shimojima, K. Ishizaka, Y. Ishida, N. Katayama, K. Ohgushi, T. Kiss, M. Okawa, T. Togashi, X.-Y. Wang, C.-T. Chen, S. Watanabe, R. Kadota, T. Oguchi, A. Chainani, and S. Shin, Orbital-dependent modifications of electronic structure across the magnetostructural transition in $BaFe_2As_2$, Phys. Rev. Lett. **104**, 057002 (2010).
[63] J. M. Caron, J. R. Neilson, D. C. Miller, K. Arpino, A. Llobet, and T. M. McQueen, Orbital-selective magnetism in the spin-ladder iron selenides $Ba_{1-x}K_xFe_2Se_3$, Phys. Rev. B **85**, 180405(R) (2012).
[64] Z. P. Yin, Kristjan Haule, and Gabriel Kotliar, Kinetic frustration and the nature of the magnetic and paramagnetic states in iron pnictides and iron chalcogenides, Nat. Mater. **10**, 932 (2011).
[65] Yu Li, Zhiping Yin, Xiancheng Wang, David W. Tam, D. L. Abernathy, A. Podlesnyak, Chenglin Zhang, Meng Wang, Lingyi Xing, Changqing Jin, Kristjan Haule, Gabriel Kotliar, Thomas A. Maier, and Pengcheng Dai, Orbital selective spin excitations and their impact on superconductivity of $LiFe_{1-x}Co_xAs$, Phys. Rev. Lett. **116**, 247001 (2016).
[66] Lara Benfatto, Belén Valenzuela, and Laura Fanfarillo, Nematic pairing from orbital-selective spin fluctuations in FeSe, npj Quantum Mater. **3**, 1 (2018).
[67] J. Herbrych, Nitin Kaushal, Alberto Nocera, Gonzalo Alvarez, Adriana Moreo, and E. Dagotto, Spin dynamics of the block orbital-selective Mott phase, Nat. Commun. **9**, 1 (2018).
[68] N. D. Patel, A. Nocera, G. Alvarez, A. Moreo, S. Johnston, and E. Dagotto, Fingerprints of an orbital-selective Mott phase in the block magnetic state of $BaFe_2Se_3$ ladders, Commun. Phys. **2**, 1 (2019).
[69] David W. Tam, Zhiping Yin, Yaofeng Xie, Weiyi Wang, M. B. Stone, D. T. Adroja, H. C. Walker, Ming Yi, and Pengcheng Dai, Orbital selective spin waves in detwinned NaFeAs, Phys. Rev. B **102**, 054430 (2020).
[70] Yang Zhang, Ling-Fang Lin, Gonzalo Alvarez, Adriana Moreo, and Elbio Dagotto, Magnetic states of the quasi-one-dimensional iron chalcogenide Ba_2FeS_3, Phys. Rev. B **104**, 125122 (2021).
[71] Ling-Fang Lin, Yang Zhang, Gonzalo Alvarez, Adriana Moreo, and Elbio Dagotto, Origin of insulating ferromagnetism in iron oxychalcogenide $Ce_2O_2FeSe_2$, Phys. Rev. Lett. **127**, 077204 (2021).
[72] Ling-Fang Lin, Yang Zhang, Gonzalo Alvarez, Jacek Herbrych, Adriana Moreo, and Elbio Dagotto, Prediction of orbital-selective Mott phases and block magnetic states in the quasi-one-dimensional iron chain $Ce_2O_2FeSe_2$ under hole and electron doping, Phys. Rev. B **105**, 075119 (2022).
[73] Evgeny A. Stepanov, Yusuke Nomura, Alexander I. Lichtenstein, and Silke Biermann, Orbital isotropy of magnetic fluctuations in correlated electron materials induced by Hund's exchange coupling, Phys. Rev. Lett. **127**, 207205 (2021).
[74] Antoine Georges, Gabriel Kotliar, Werner Krauth, and Marcelo J. Rozenberg, Dynamical mean-field theory of

strongly correlated fermion systems and the limit of infinite dimensions, Rev. Mod. Phys. **68**, 13 (1996).
[75] T. A. Maier, Mark Jarrell, Thomas Pruschke, and M. Hettler, Quantum cluster theories, Rev. Mod. Phys. **77**, 1027 (2005).
[76] Thomas Schäfer *et al.*, Tracking the footprints of spin fluctuations: A MultiMethod, MultiMessenger study of the two-dimensional Hubbard model, Phys. Rev. X **11**, 011058 (2021).
[77] Connor Lenihan, Aaram J. Kim, Fedor Šimkovic, and Evgeny Kozik, Evaluating second-order phase transitions with diagrammatic Monte Carlo: Néel transition in the doped three-dimensional Hubbard model, Phys. Rev. Lett. **129**, 107202 (2022).
[78] M. Vandelli, Quantum embedding methods in dual space for strongly interacting electronic systems, Ph.D. thesis, Universität Hamburg, Hamburg, 2022.
[79] E. A. Stepanov, V. Harkov, and A. I. Lichtenstein, Consistent partial bosonization of the extended Hubbard model, Phys. Rev. B **100**, 205115 (2019).
[80] V. Harkov, M. Vandelli, S. Brener, A. I. Lichtenstein, and E. A. Stepanov, Impact of partially bosonized collective fluctuations on electronic degrees of freedom, Phys. Rev. B **103**, 245123 (2021).
[81] Matteo Vandelli, Josef Kaufmann, Mohammed El-Nabulsi, Viktor Harkov, Alexander I. Lichtenstein, and Evgeny A. Stepanov, Multi-band D-TRILEX approach to materials with strong electronic correlations, SciPost Phys. **13**, 036 (2022).
[82] Thomas Ayral and Olivier Parcollet, Mott physics and spin fluctuations: A unified framework, Phys. Rev. B **92**, 115109 (2015).
[83] Thomas Ayral and Olivier Parcollet, Mott physics and spin fluctuations: A functional viewpoint, Phys. Rev. B **93**, 235124 (2016).
[84] A. N. Rubtsov, M. I. Katsnelson, and A. I. Lichtenstein, Dual fermion approach to nonlocal correlations in the Hubbard model, Phys. Rev. B **77**, 033101 (2008).
[85] A. N. Rubtsov, M. I. Katsnelson, A. I. Lichtenstein, and A. Georges, Dual fermion approach to the two-dimensional Hubbard model: Antiferromagnetic fluctuations and Fermi arcs, Phys. Rev. B **79**, 045133 (2009).
[86] H. Hafermann, G. Li, A. N. Rubtsov, M. I. Katsnelson, A. I. Lichtenstein, and H. Monien, Efficient perturbation theory for quantum lattice models, Phys. Rev. Lett. **102**, 206401 (2009).
[87] Sergey Brener, Evgeny A. Stepanov, Alexey N. Rubtsov, Mikhail I. Katsnelson, and Alexander I. Lichtenstein, Dual fermion method as a prototype of generic reference-system approach for correlated fermions, Ann. Phys. (Amsterdam) **422**, 168310 (2020).
[88] A. N. Rubtsov, M. I. Katsnelson, and A. I. Lichtenstein, Dual boson approach to collective excitations in correlated fermionic systems, Ann. Phys. (Amsterdam) **327**, 1320 (2012).
[89] Erik G. C. P. van Loon, Alexander I. Lichtenstein, Mikhail I. Katsnelson, Olivier Parcollet, and Hartmut Hafermann, Beyond extended dynamical mean-field theory: Dual boson approach to the two-dimensional extended Hubbard model, Phys. Rev. B **90**, 235135 (2014).
[90] E. A. Stepanov, E. G. C. P. van Loon, A. A. Katanin, A. I. Lichtenstein, M. I. Katsnelson, and A. N. Rubtsov, Self-consistent dual boson approach to single-particle and collective excitations in correlated systems, Phys. Rev. B **93**, 045107 (2016).
[91] E. A. Stepanov, A. Huber, E. G. C. P. van Loon, A. I. Lichtenstein, and M. I. Katsnelson, From local to nonlocal correlations: The dual boson perspective, Phys. Rev. B **94**, 205110 (2016).
[92] E. A. Stepanov, S. Brener, F. Krien, M. Harland, A. I. Lichtenstein, and M. I. Katsnelson, Effective Heisenberg model and exchange interaction for strongly correlated systems, Phys. Rev. Lett. **121**, 037204 (2018).
[93] E. A. Stepanov, A. Huber, A. I. Lichtenstein, and M. I. Katsnelson, Effective Ising model for correlated systems with charge ordering, Phys. Rev. B **99**, 115124 (2019).
[94] L. Peters, E. G. C. P. van Loon, A. N. Rubtsov, A. I. Lichtenstein, M. I. Katsnelson, and E. A. Stepanov, Dual boson approach with instantaneous interaction, Phys. Rev. B **100**, 165128 (2019).
[95] M. Vandelli, V. Harkov, E. A. Stepanov, J. Gukelberger, E. Kozik, A. Rubio, and A. I. Lichtenstein, Dual boson diagrammatic Monte Carlo approach applied to the extended Hubbard model, Phys. Rev. B **102**, 195109 (2020).
[96] E. A. Stepanov, S. Brener, V. Harkov, M. I. Katsnelson, and A. I. Lichtenstein, Spin dynamics of itinerant electrons: Local magnetic moment formation and Berry phase, Phys. Rev. B **105**, 155151 (2022).
[97] E. A. Stepanov, V. Harkov, M. Rösner, A. I. Lichtenstein, M. I. Katsnelson, and A. N. Rudenko, Coexisting charge density wave and ferromagnetic instabilities in monolayer InSe, npj Comput. Mater. **8**, 118 (2022).
[98] M. Vandelli, A. Galler, A. Rubio, A. I. Lichtenstein, S. Biermann, and E. A. Stepanov, Doping-dependent charge- and spin-density wave orderings in a monolayer of Pb adatoms on Si(111), npj Quantum Mater. **9**, 19 (2024).
[99] Maria Chatzieleftheriou, Silke Biermann, and Evgeny A. Stepanov, Local and nonlocal electronic correlations at the metal-insulator transition in the Hubbard model in two dimensions, arXiv:2312.03123.
[100] Evgeny A. Stepanov, Maria Chatzieleftheriou, Niklas Wagner, and Giorgio Sangiovanni, Interconnected renormalization of Hubbard bands and Green's function zeros in Mott insulators induced by strong magnetic fluctuations, arXiv:2402.02814.
[101] G. Rohringer, H. Hafermann, A. Toschi, A. A. Katanin, A. E. Antipov, M. I. Katsnelson, A. I. Lichtenstein, A. N. Rubtsov, and K. Held, Diagrammatic routes to nonlocal correlations beyond dynamical mean field theory, Rev. Mod. Phys. **90**, 025003 (2018).
[102] Ya. S. Lyakhova, G. V. Astretsov, and A. N. Rubtsov, The mean-field concept and post-DMFT methods in the contemporary theory of correlated systems, Phys-Usp, **193**, 825 (2023); **66**, 775 (2023).
[103] M. Vandelli, J. Kaufmann, V. Harkov, A. I. Lichtenstein, K. Held, and E. A. Stepanov, Extended regime of metastable metallic and insulating phases in a two-orbital electronic system, Phys. Rev. Res. **5**, L022016 (2023).

[104] Evgeny A. Stepanov, Matteo Vandelli, Alexander I. Lichtenstein, and Frank Lechermann, Charge density wave ordering in $NdNiO_2$: Effects of multiorbital nonlocal correlations, arXiv:2311.09983.

[105] See Supplemental Material at http://link.aps.org/supplemental/10.1103/PhysRevLett.132.226501 for the Néel temperature for different values of Hund's coupling.

[106] Lars Hedin, New method for calculating the one-particle Green's function with application to the electron-gas problem, Phys. Rev. **139**, A796 (1965).

[107] Massimo Capone, Michele Fabrizio, Paolo Giannozzi, and Erio Tosatti, Theory of the metal-nonmagnetic Mott-Jahn-Teller insulator transition in A_4C_{60}, Phys. Rev. B **62**, 7619 (2000).

[108] Massimo Capone, Michele Fabrizio, and Erio Tosatti, Direct transition between a singlet Mott insulator and a superconductor, Phys. Rev. Lett. **86**, 5361 (2001).

[109] Yusuke Nomura, Shiro Sakai, Massimo Capone, and Ryotaro Arita, Unified understanding of superconductivity and Mott transition in alkali-doped fullerides from first principles, Sci. Adv. **1**, e1500568 (2015).

[110] Massimo Capone, Michele Fabrizio, Claudio Castellani, and Erio Tosatti, Colloquium: Modeling the unconventional superconducting properties of expanded A_3C_{60} fullerides, Rev. Mod. Phys. **81**, 943 (2009).

[111] Minjae Kim, Yusuke Nomura, Michel Ferrero, Priyanka Seth, Olivier Parcollet, and Antoine Georges, Enhancing superconductivity in A_3c_{60} fullerides, Phys. Rev. B **94**, 155152 (2016).

[112] Daniel Hirschmeier, Hartmut Hafermann, Emanuel Gull, Alexander I. Lichtenstein, and Andrey E. Antipov, Mechanisms of finite-temperature magnetism in the three-dimensional Hubbard model, Phys. Rev. B **92**, 144409 (2015).